Adsorption of Globular Proteins on Locally Planar Surfaces. II. Models for the Effect of Multiple Adsorbate Conformations on Adsorption Equilibria and Kinetics

Allen P. Minton
Section on Physical Biochemistry, Laboratory of Biochemistry and Genetics, National Institute of Diabetes and Digestive and Kidney Diseases, National Institutes of Health, Bethesda, Maryland 20892-0830 USA

ABSTRACT Equilibrium and kinetic models for nonspecific adsorption of proteins to planar surfaces are presented. These models allow for the possibility of multiple interconvertible surface conformations of adsorbed protein. Steric repulsion resulting in area exclusion by adsorbed molecules is taken into account by treating the adsorbate as a thermodynamically nonideal two-dimensional fluid. In the equilibrium model, the possibility of attractive interactions between adsorbed molecules is taken into account in a limited fashion by permitting one of the adsorbed species to self-associate. Calculated equilibrium adsorption isotherms exhibit apparent high-affinity and low-affinity binding regions, corresponding respectively to adsorption of ligand at low fractional area occupancy in an energetically favorable side-on conformation and conversion at higher fractional area occupancy of the side-on conformation to an entropically favored end-on conformation. Adsorbate self-association may lead to considerable steepening of the adsorption isotherm, compensating to a variable extent for the broadening effect of steric repulsion. Kinetic calculations suggest that in the absence of attractive interactions between adsorbate molecules, the process of adsorption may be highly "stretched" along the time axis, rendering the attainment of adsorption equilibrium in the context of conventional experiments problematic.

INTRODUCTION

When the potential of interaction between a soluble macromolecule ("ligand") and a surface depends strongly upon position within the plane of the surface, it is conventional to analyze interactions between ligand and the surface in the context of models for binding of ligand to discrete sites (see for example, Boeynaems and Dumont, 1980). In the present work, as in the preceding work in this series (Chatelier and Minton, 1996), referred to herein as CM, we shall be concerned with interactions between surface and ligand that are to a good approximation independent of position in the plane of the surface, i.e., depend primarily upon the distance between the surface and the ligand molecule, and, in the present work, on the orientation of the ligand molecule relative to the surface (Roth and Lenhoff, 1993; Roush et al., 1994). Interactions of this type are commonly assumed to underlie phenomena such as the nonspecific adsorption of macromolecules to synthetic or naturally occurring phospholipid membranes (Heimburg and Marsh, 1995), the surfaces of particles of synthetic polymers (Al-Malah et al., 1995), or a "molecularly flat" (see Note 1) surface of any large array of molecular species whose cross-sectional area in the plane of the surface is significantly smaller than that of an adsorbed ligand molecule. Prior theoretical analysis and modeling of such systems have indicated that steric repulsions between adsorbed ligands lead to marked broadening of the equilibrium adsorption isotherm relative to that characteristic of homogeneous independent site binding (Heimburg and Marsh, 1995; Chatelier and Minton, 1996), as well as greatly increasing the length of time required to attain steady state at high fractional surface coverage (Jin et al., 1994; Kurrat et al., 1997).

Experimental studies of protein adsorption have suggested the possibility that proteins may adsorb in more than a single conformation, and that the probability of adsorbing in a given conformation may vary with the surface density of adsorbed protein (Brynda et al., 1986; Wahlgren et al., 1995). Talbot has recently presented a hard particle equilibrium model for such a phenomenon (Talbot, 1997). In the present paper we present a model that is similar in concept to that of Talbot, but which has been extended to treat the kinetic as well as equilibrium aspects of multiple adsorbate conformations, and also to explore the consequences of self-association of one of the adsorbate conformations.

THEORY AND RESULTS: EQUILIBRIUM

The chemical potential of a single ligand species behaving ideally in solution is given by

$$\mu^{\mathrm{soln}} = \mu^{\mathrm{soln,o}} + RT \ln c \qquad (1)$$

where $\mu^{\mathrm{soln,o}}$ denotes the standard state chemical potential of ligand, c its concentration in solution, R the molar gas constant, and T the absolute temperature. Let us postulate that adsorbed ligand ("adsorbate") may be present in any of i possible conformations. The chemical potential of the ith adsorbate conformation is given by

$$\mu_{\mathrm{i}}^{\mathrm{surf}} = \mu_{\mathrm{i}}^{\mathrm{surf,o*}} + RT \ln \phi_{\mathrm{i}} + RT \ln \gamma_{\mathrm{i}}(\{\phi\}) \qquad (2)$$

Received for publication 23 June 1998 and in final form 14 September 1998.

Address reprint requests to Dr. Allen P. Minton, Building 8, Room 226, National Institutes of Health, Bethesda, MD 20892-0830. Tel.: 301-496-3604; Fax: 301-402-0240; E-mail: minton@helix.nih.gov.

0006-3495/99/01/176/12 $2.00

where $\mu_i^{surf,o*}$ denotes the standard state of the ith conformation of adsorbate, ϕ_i the fraction of surface area occupied by adsorbate in conformation i, and γ_i the activity coefficient of the ith conformation, here indicated as a function of the fractional area occupancies of all adsorbate conformations. We shall refer to the cross section of the ith adsorbate conformation in the plane of the surface as its "footprint," and denote the area and circumference of the footprint by a_i and s_i, respectively. Then the number density of species i will be given by

$$\rho_i = \phi_i/a_i \tag{3a}$$

and Eq. 2 may be rewritten as

$$\mu_i^{surf} = \mu_i^{surf,o} + RT \ln \rho_i + RT \ln \gamma_i(\{\rho\}) \tag{3b}$$

where $\mu_i^{surf,o} \equiv \mu_i^{surf,o*} + \text{RT ln } a_i$. The condition of adsorption equilibrium is given by

$$\mu^{soln} = \mu_i^{surf} \tag{4}$$

for all i. By combining Eqs. 1, 3, and 4 we obtain a set of equations

$$K_i c = \rho_i \gamma_i(\{\rho\}) \tag{5}$$

where

$$K_i \equiv \exp\left[\frac{-(\mu_i^{surf,o} - \mu^{soln,o})}{RT}\right] \tag{6}$$

is an "intrinsic" coefficient for the partitioning of ligand between solution and surface species i in the limit of low surface density of adsorbed ligand ($\gamma_i = 1$ for all i).

It has been demonstrated that under experimental conditions such that intermolecular interactions other than steric exclusion are damped out (moderate ionic strength, pH $\sim$ pI), the concentration dependence of colligative properties of protein solutions may be well accounted for by simple models in which protein molecules are represented by convex hard particles (Zimmerman and Minton, 1993). Hard particles have also been used to model the adsorption of macromolecules (Jin et al., 1994; Heimburg and Marsh, 1995; Chatelier and Minton, 1996; Sild et al., 1996). In the present work we formulate a simple hard particle model for multiple adsorbate conformations, illustrated schematically in Fig. 1, in which the adsorbing macromolecule is represented as a hard rectangular parallelopiped (HRP) of dimensions $r \times r \times Lr$ (axial ratio L). This particle may adsorb in the "side-on" conformation (species 1), with a rectangular footprint of dimensions $r \times Lr$, or in the "end-on" conformation (species 2), with a square footprint of dimensions $r \times r$. It may be readily shown that all dimensions may be scaled to r, with no change to the above equations other than in the numerical value of $\mu_i^{surf,o}$ (and hence K_i). For convenience in calculation we shall henceforth set $r = 1$ with no loss in generality. Thus $a_1 = L$, $s_1 = 2(1 + L)$, $a_2 = 1$, and $s_2 = 4$.

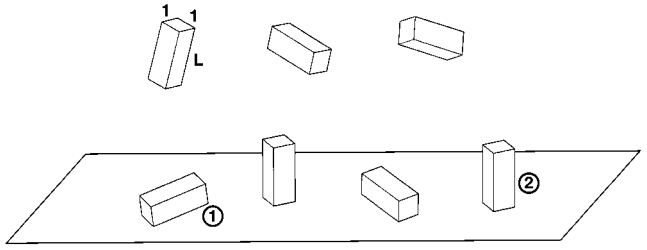

FIGURE 1 Model for adsorption in multiple surface conformations. Ligand is depicted as a hard rectangular parallelopiped of dimensions $1 \times 1 \times L$ that may adsorb onto a planar surface in a side-on (1) or end-on (2) conformation.

In this simple model, the "intrinsic" free energy of adsorption of each conformation is assumed to be proportional to the footprint area and to vary with the degeneracy d of the conformation (see Note 2).

$$\frac{\Delta G_i^o}{RT} = -\ln K_i = -Ja_i - \ln d_i \tag{7}$$

where J is the adsorption potential, in units of RT per unit footprint area, $d_1 = 4$, and $d_2 = 2$. It follows from Eqs. 4 or 5 and 7 that one may define a constant of equilibrium between adsorbate conformations 1 and 2:

$$K_{21} \equiv \frac{K_1}{K_2} = \frac{\gamma_1(\{\rho\})\rho_1}{\gamma_2(\{\rho\})\rho_2} = \frac{d_1 \exp(Ja_1)}{d_2 \exp(Ja_2)} \tag{8}$$

The activity coefficient of a particular adsorbate conformation is calculated using a relation due to Talbot (Talbot et al., 1994) derived from scaled particle theory for a mixture of hard convex particles in two dimensions:

$$\ln \gamma_i(\{\rho\}) = -\ln(1 - \langle \rho a \rangle) + \frac{a_i\langle \rho \rangle + s_i\langle \rho s \rangle/(2\pi)}{1 - \langle \rho a \rangle} + \frac{a_i}{4\pi}\left[\frac{\langle \rho s \rangle}{1 - \langle \rho a \rangle}\right]^2 \tag{9}$$

where $\langle \rho \rangle \equiv \Sigma \rho_j$, $\langle \rho a \rangle \equiv \Sigma \rho_j a_j$, and $\langle \rho s \rangle \equiv \Sigma \rho_j s_j$.

This equilibrium model may be extended to allow for the self-association of end-on adsorbate molecules, illustrated schematically in Fig. 2. Let adsorbate species 3 be the n-mer of the end-on species 2, with a square footprint (see Note 3). According to this model, $a_3 = n$, $s_3 = 4\sqrt{n}$, and $d_3 = 2$. We define the equilibrium constant for the formation of adsorbate species 3:

$$K_{23} \equiv \frac{\gamma_3(\{\rho\})\rho_3}{(\gamma_2(\{\rho\})\rho_2)^n} \tag{10}$$

Given values of J, L, K_{23}, and the a_i, s_i, and d_i, one may calculate the equilibrium values of ρ_i and ϕ_i (and hence $\rho_{tot} = \Sigma \rho_i$ and $\phi_{tot} = \Sigma \phi_i$) as functions of $K_2 c$ via iterative numerical solution of Eqs. 1, 4, 5, and 8–10 (see Note 4).

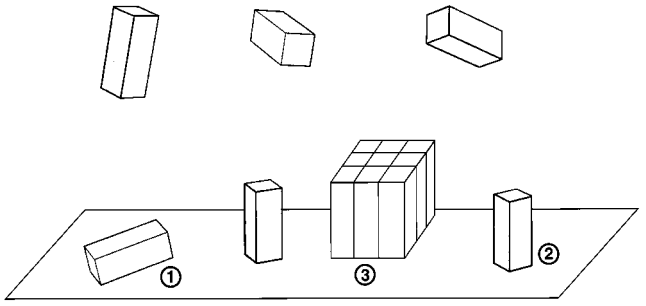

FIGURE 2 Model for an adsorption in multiple surface conformations, allowing for the possibility of self-association of adsorbed ligand. Adsorbate species (1) and (2) are as defined in the caption of Fig. 1. Adsorbate species (3) is an *n*-mer of species (2) that is assumed to have a square footprint with an area corresponding to *n* times that of the monomer.

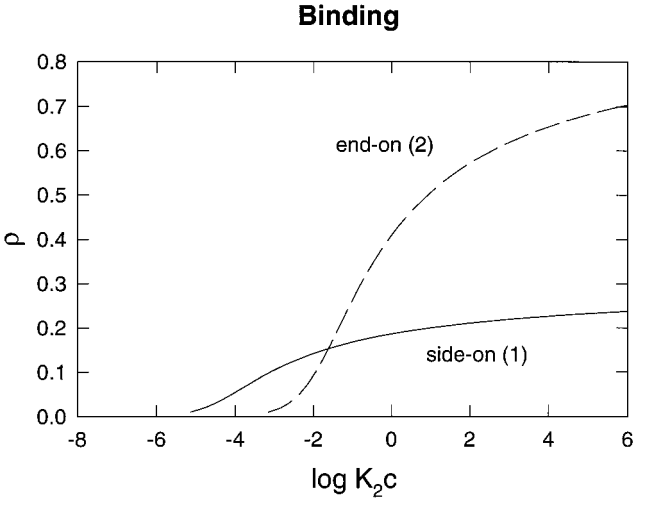

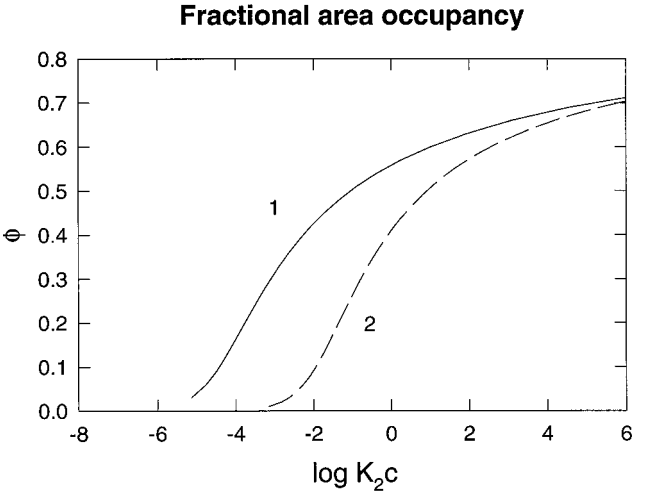

FIGURE 3 Equilibrium adsorption isotherms for ligand that can adsorb in either side-on or end-on conformation exclusively (*solid* and *dashed curves*, respectively), calculated as described in the text with $J = 2$, $L = 3$, and $K_{23} = 0$. Isotherms in this figure differ from those plotted in subsequent figures in that adsorbate is present in only a single conformation that is not allowed to equilibrate with any other conformation. Results are presented as relative amount adsorbed (*top panel*) and fraction of surface area occupied (*bottom panel*). Normalized free ligand concentrations *Kc* in this figure as well as Figs. 4–9 are set equal to K_2c.

Some effects of multiple adsorption conformations on the adsorption equilibrium of a single solution species are depicted in Figs. 3–9. It is instructive to plot both the relative amount and the fractional surface coverage of each adsorbed species as functions of the normalized concentration of free ligand. For reference, in Fig. 3 we plot the adsorption isotherms of HRPs that are allowed to bind only in a single conformation, either side-on (1) or end-on (2); no equilibration between conformations is permitted. These isotherms are identical, in the case of conformation 2, or similar, in the case of conformation 1, to isotherms presented in Fig. 1 of CM. The side-on conformation has an intrinsically higher affinity because it has both a larger contact area (assumed proportional to binding potential) as well as a greater degeneracy than the end-on conformation.

In Fig. 4 the side-on and end-on conformations are allowed to equilibrate, and the activity coefficients of each conformation depends upon the number densities of both conformations, as specified by Eq. 9. The adsorption isotherm exhibits apparent high-affinity and low-affinity adsorption regions. The high-affinity region corresponds to the adsorption of ligand in the side-on conformation that is energetically favored at low fractional surface occupancy. As fractional surface coverage increases with increasing ligand concentration, the activity coefficient of the side-on conformation (larger footprint) increases so much more rapidly than that of the end-on conformation (smaller footprint) that the equilibrium between side-on and end-on (Eq. 8) shifts in favor of the now entropically favored end-on mode. The conversion of side-on to end-on and subsequent addition of ligand in the end-on conformation is manifested as a lower-affinity adsorption process. In Figs. 5 and 6 the effects of increasing the adsorption potential and increasing the axial ratio of ligand are plotted. These two variations have qualitatively similar effects, because increasing either parameter results in an enhancement of the intrinsic affinity of the side-on conformation relative to that of the end-on conformation. We note that when the energetic difference between side-on and end-on configurations becomes sufficiently great, a region appears in the adsorption isotherm where the fractional surface coverage is predicted to decrease, rather than increase, with increasing free ligand concentration. This counterintuitive result, previously noted by Talbot (1997), occurs whenever an increase in free ligand concentration results in more conversion of larger-footprint conformation 1 to smaller-footprint conformation 2 than adsorption of additional ligand from solution.

In Fig. 7 the effect of self-association of end-on conformation 2 on the adsorption isotherm is illustrated. Since the *n*-meric conformation 3 excludes even less area per molecule of adsorbate than monomeric conformation 2, area exclusion tends to promote the formation of 3, and conformation 2 does not accumulate to a major extent at equilibrium. In Fig. 8 the effect of altering K_{23} for a constant

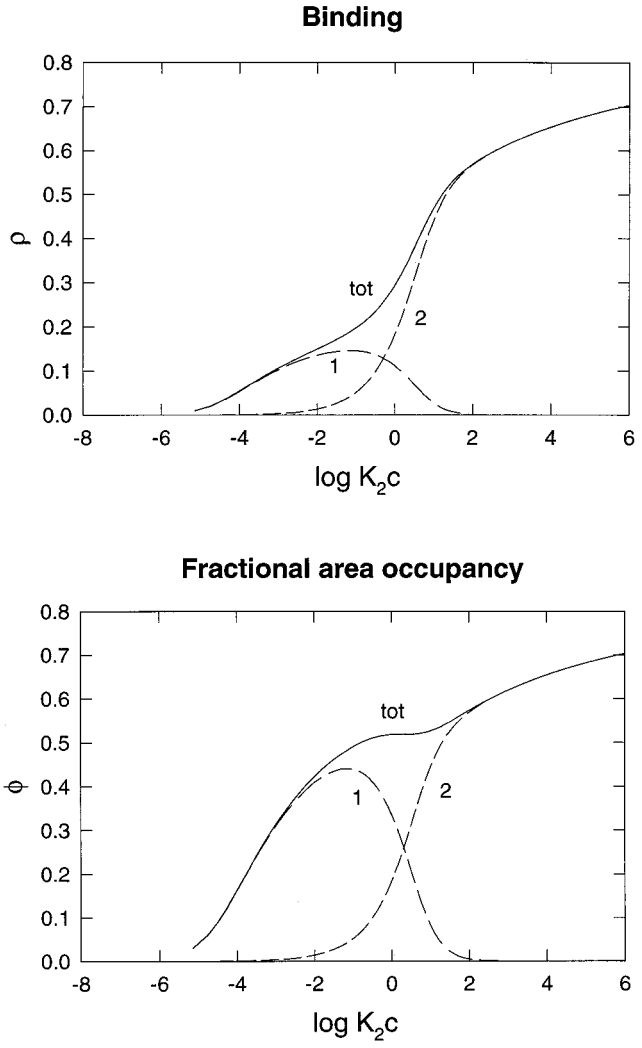

FIGURE 4 Equilibrium adsorption isotherm of a ligand adsorbing in two interconverting conformations. Model parameters as in Fig. 3. Plotted curves indicate the relative amount of adsorbate (*top panel*) and fraction of surface area occupied (*bottom panel*) for total adsorbate (*solid curve*) and individual adsorbate species (*dashed curves*).

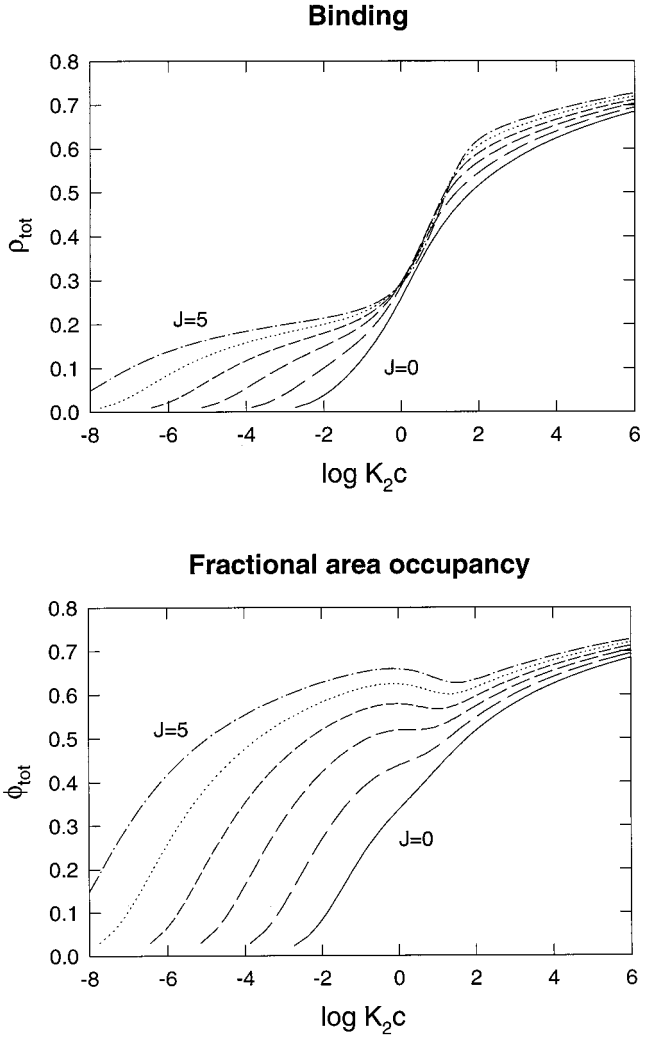

FIGURE 5 Effect of variation in intrinsic binding potential per unit footprint area on total adsorption. Isotherms are calculated for $L = 3$, $K_{23} = 0$, and $J = 0$, 1, 2, 3, 4, and 5 (*rightmost* to *leftmost curves*). Panels as in preceding figures.

degree of oligomerization ($n = 4$) is illustrated, and in Fig. 9 the effect of altering the degree of oligomerization for a constant value of K_{23} is illustrated. As the value of n increases, the maximal equilibrium abundance of end-on monomer becomes vanishingly small, and the adsorption isotherm approaches the behavior characteristic of a first-order phase transition; all ligand adsorbed in excess of the "solubility limit" (in this example, $\rho_{sol} \sim 0.2$) is incorporated into a two-dimensional quasi-crystalline array (i.e., conformation 3 in the limit of large n). Similar behavior was predicted earlier by CM using a model in which hard circular adsorbate particles could equilibrate with an oligomeric adsorbate modeled by a larger hard circle.

THEORY AND RESULTS: KINETICS

The following is a simple model for the time dependence of adsorption in the absence of adsorbate oligomerization (see Note 5). We individually consider the following elementary processes.

1. *Adsorption of conformational species i from the supernatant solution.* The overall rate is the product of the intrinsic encounter rate, $k_a^o c$, the degeneracy of species i, d_i, and the probability that a randomly selected element of surface area with the dimensions of the footprint of i is vacant, P_i. For a hard particle model, $P_i = 1/\gamma_i(\{\rho\})$ (Lebowitz et al., 1965) (see Note 6). Hence

$$\text{rate}_{\text{soln}\rightarrow i} = k_a^o\, c\, d_i/\gamma_i(\{\rho\}) \tag{11}$$

2. *Desorption of conformational species i.* The overall rate is the product of an intrinsic desorption rate constant times a Boltzmann factor, $B_i = \exp(-Ja_i)$, reflecting the additional energy required for conformation i to escape the adsorption potential well.

$$\text{rate}_{i\rightarrow\text{soln}} = k_d^o \rho_i \exp(-Ja_i) \tag{12}$$

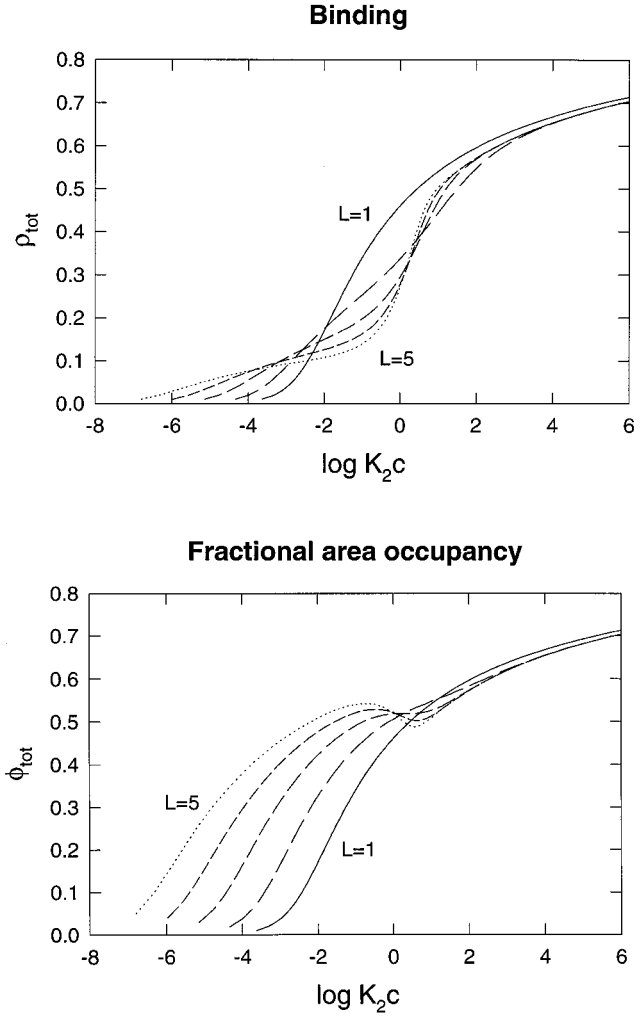

FIGURE 6 Effect of variation in shape of ligand shape on total adsorption. Isotherms are calculated for $J = 2$, $K_{23} = 0$, and $L = 1$, 2, 3, 4, and 5 (*solid* to *dotted curves*, respectively).

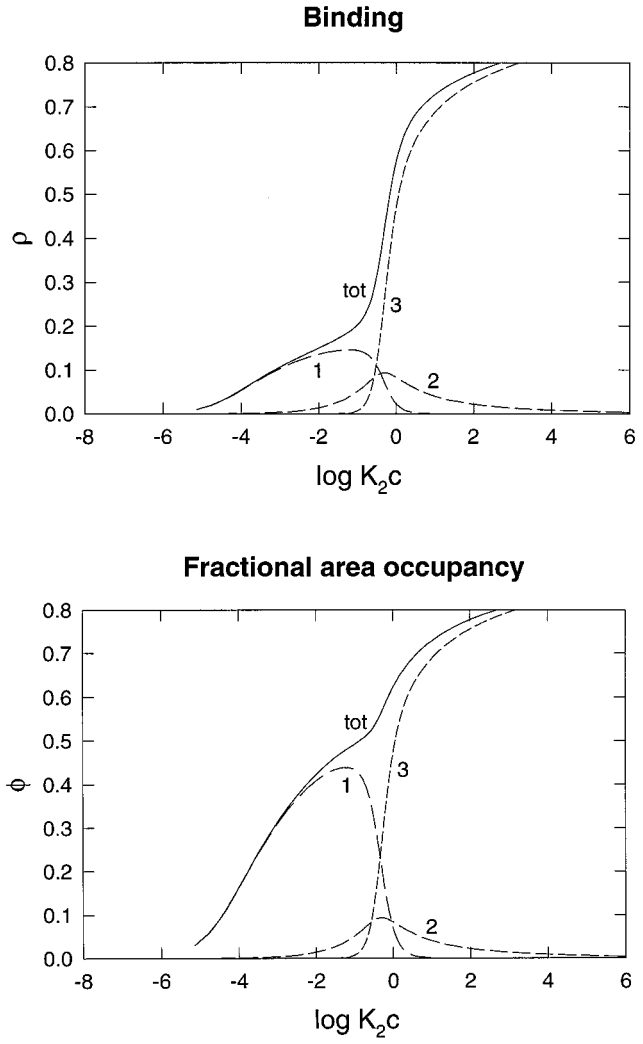

FIGURE 7 Equilibrium adsorption of a ligand with three interconverting adsorbate conformations, calculated for $J = 2$, $L = 3$, $K_{23} = 1$, and $n = 4$. Plotted curves indicate the relative amount of adsorbate (*top panel*) and fraction of surface area occupied (*bottom panel*) for total adsorbate (*solid curve*) and individual adsorbate species (*dashed curves*).

3. *Adsorbate "flipping,"* i.e., conversion of conformation i to conformation j ($1 \rightarrow 2$ or $2 \rightarrow 1$) without total desorption. We estimate this rate using simple transition state rate theory (Hill, 1960), according to which

$$\text{rate}_{i\rightarrow j}^{\text{flip}} = \rho_T k_{\text{dec}}^{o} f_j \tag{13}$$

where ρ_T is the steady-state concentration of transition state T, k_{dec}^{o} is the intrinsic decay rate of T, and f_j is the fraction of T that decays to adsorbate conformation j rather than back to i. Let the adsorption energy of the transition state T, which is smaller in magnitude than that of either conformation 1 or 2, be denoted by x. Then $\rho_T = \rho_i \exp(-(Ja_i - x)) = \rho_i \exp(-Ja_i)\exp(x)$. f_j is the product of two independent probabilities, $P_{T\rightarrow j}^{(1)} = d_j/(d_i + d_j)$, representing the probability of T decaying to j in the absence of surface area exclusion (low occupancy limit), and $P_{T\rightarrow j}^{(2)} \approx P_j/(P_i + P_j)$, representing the effect of excluded area on the relative likelihood of successful surface placement of an additional molecule in each of the conformational states. Substitution of these terms into Eq. 13 yields the approximate expression

$$\text{rate}_{i\rightarrow j}^{\text{flip}} = k_{\text{flip}}^{*}\rho_i \exp(-Ja_i)\frac{d_j}{d_i + d_j}\frac{\gamma_i(\{\rho\})}{\gamma_i(\{\rho\}) + \gamma_j(\{\rho\})} \tag{14}$$

where $k_{\text{flip}}^{*} \equiv k_{\text{dec}}^{o} \exp(x)$.

The overall time dependence of binding is given by

$$\rho_{tot}(t) = \rho_1(t) + \rho_2(t) \tag{15}$$

where

$$\rho_i(t) = \rho_i(t = 0) + \int_0^t \frac{d\rho_i}{dt}(t')\,dt' \tag{16}$$

and

$$d\rho_i/dt = \text{rate}_{\text{soln}\rightarrow i} + \text{rate}_{j\rightarrow i}^{\text{flip}} - \text{rate}_{i\rightarrow j}^{\text{flip}} - \text{rate}_{i\rightarrow \text{soln}} \tag{17}$$

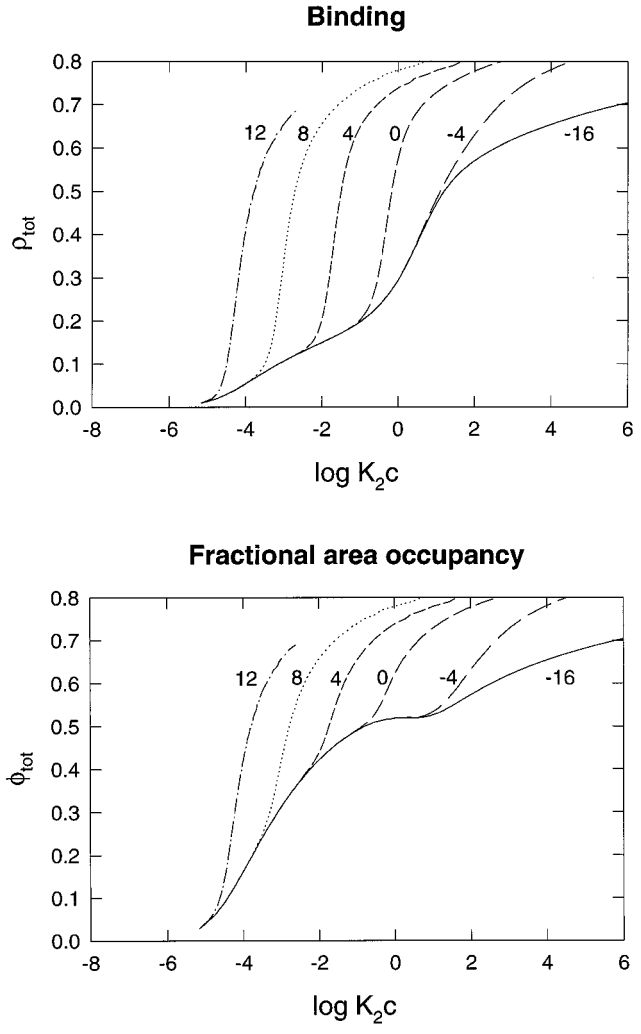

FIGURE 8 Effect of variation in adsorbate self-association equilibrium constant upon total equilibrium adsorption, calculated for $J = 2$, $L = 3$, $n = 4$, and $K_{23} = 10^{-16}$, 10^{-4}, 1, 10^4, 10^8 and 10^{12} (curves shift progressively leftward with increasing K_{23}).

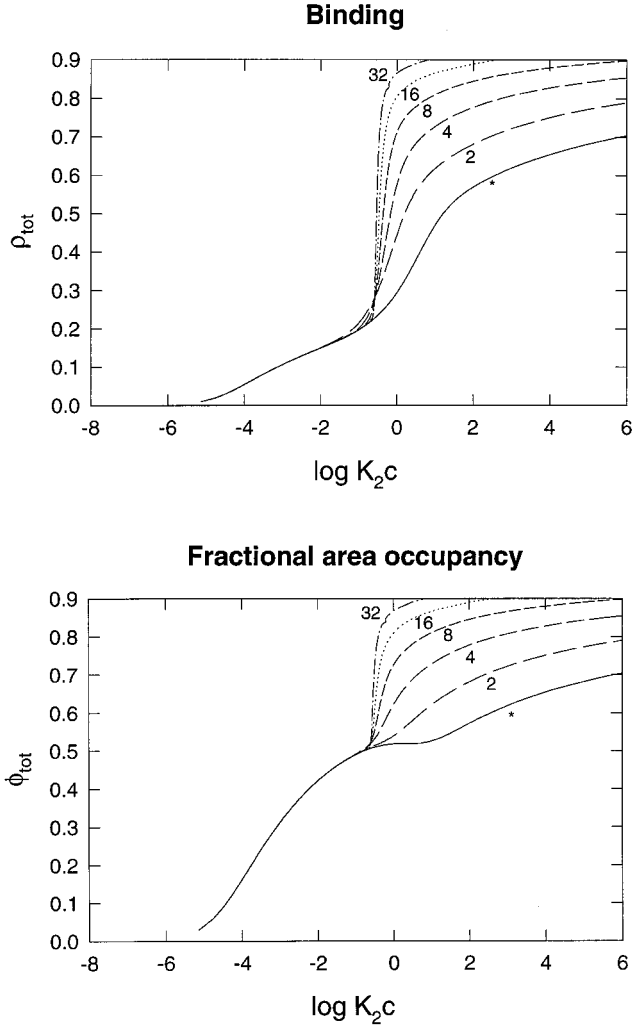

FIGURE 9 Effect of variation in degree of self-association upon total equilibrium adsorption, calculated for $J = 2$, $L = 3$, $K_{23} = 1$, and $n = 1$, 2, 4, 8, 16, and 32 (curves shift progressively leftward and become steeper with increasing n).

To simplify calculation, let us define the scaled time $t^* \equiv k_d^o t$. Then it follows from Eqs. 11, 12, 14, and 17 that

$$\frac{d\rho_i}{dt^*} = \frac{Kcd_i}{\gamma_i(\{\rho\})} - \rho_i \exp(-Ja_i) + k_{flip}\left[\frac{\rho_j \exp(-Ja_j) d_i \gamma_j(\{\rho\}) - \rho_i \exp(-Ja_i) d_j \gamma_i(\{\rho\})}{(d_i + d_j)[\gamma_i(\{\rho\}) + \gamma_j(\{\rho\})]}\right] \quad (18)$$

where $K = k_a^o/k_d^o$ and $k_{flip} \equiv k_{flip}^*/k_d^o$ (see Note 7). $\rho_1(t^*)$, $\rho_2(t^*)$, and $\rho_{tot}(t^*)$ are obtained as functions of J, L, Kc, and k_{flip} by numerical solution of Eqs. 15, 16, and 18 using the commercially available modeling program MLAB (Civilized Software, Bethesda, MD) (see Note 8).

The time course of ρ_1, ρ_2, and ρ_{tot} calculated as described above will be compared with the conventional description of reaction kinetics in terms of sums of decaying exponentials:

$$\rho_{tot}(t^*) = \sum_j \alpha_j [1 - \exp(-t^*/t_j)] \quad (19)$$

where α_j and t_j denote, respectively, the amplitude and characteristic decay time of the contribution of the jth exponential term to total adsorption (see Note 9).

We first consider the special reference case in which ligand is permitted to adsorb in only one of the two conformations permitted by the general model, and all adsorbate remains in the single selected conformation (cf. Fig. 3). For this case, Eq. 15 reduces to

$$\rho_{tot}(t) = \rho_i(t) \quad (20)$$

where i is either 1 or 2, $\rho_j(t) = 0$ for $j \neq i$, and Eq. 18 reduces to

$$\frac{d\rho_i}{dt^*} = \frac{Kcd_i}{\gamma_i(\rho_i)} - \rho_i \exp(-Ja_i) \quad (21)$$

In the top panel of Fig. 10, adsorption progress curves are plotted for ligand adsorbing in the end-on conformation exclusively (*top panel*) and in the side-on conformation

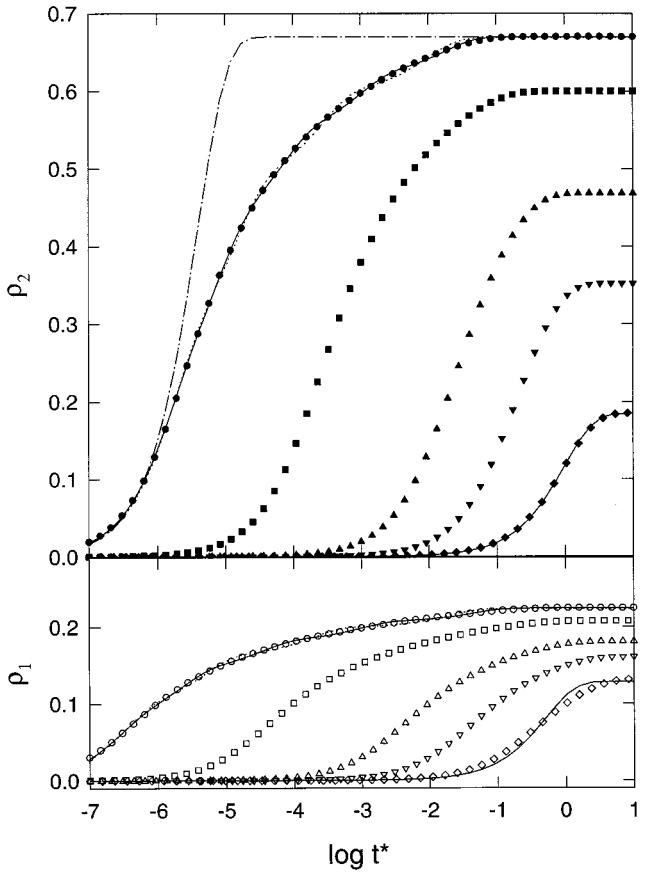

FIGURE 10 Kinetic progress curves for ligand adsorbing exclusively in the side-on conformation (*open symbols*) or in the end-on conformation (*filled symbols*), calculated for $J = 1$, $L = 3$, and $K_2c = 0.1$, 1, 10, 10^3, and 10^5 (*right* to *left*). The progress curves for $K_2c = 0.1$ are plotted together with the best fit of a single-term exponential expression of the form of Eq. 19. The progress curves for $K_2c = 10^5$ are plotted together with the best fit of a four-term exponential expression (*dotted curve*) and a five-term exponential expression (*solid curve*). Also plotted for comparison (*dot-dashed curve*) is a single exponential having the total amplitude of the progress curve for $K_2c = 10^5$ and a decay time equal to that of the initial exponential term in the multiexponential best fit.

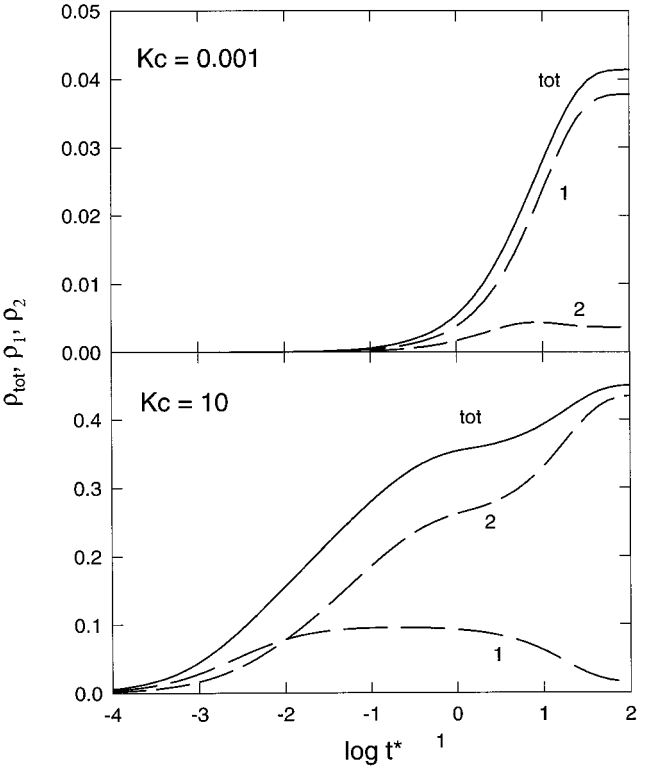

FIGURE 11 Kinetic progress curves for ligand adsorbing in side-on and end-on conformations from solution at low concentration ($K_2c = 0.001$, *top panel*) and moderately high concentration ($K_2c = 10$, *bottom panel*), calculated for $J = 1$, $L = 3$, and $k_{flip} = 0$. The relative amounts of each adsorbate conformation are plotted (*dashed lines*) together with total adsorbate (*solid lines*).

exclusively (*bottom panel*) over a wide range of free ligand concentration. In both cases, the adsorption progress curve may be described by Eq. 19 with a single term only in the limit of low free ligand concentration, i.e., low fractional surface area coverage at equilibrium. With increasing ligand concentration the progress curves become progressively broader, and at high ligand concentration the total adsorption isotherm may not be described even approximately by one or two exponential processes. We refer to adsorption progress curves such as these, in which the duration of the approach to equilibrium is substantially prolonged relative to that characteristic of an exponential process, as "stretched" progress curves. Ramifications of stretched adsorption kinetics will be discussed below.

The most important qualitative effect of area exclusion on the kinetics of multiple-mode adsorption is illustrated in Fig. 11, where the kinetics of adsorption at low fractional saturation and at high fractional saturation are contrasted. At low ligand concentration (*top panel*), the reaction starts slowly, and side-on conformation 1, with a higher intrinsic affinity than end-on conformation 2, accounts for the bulk of adsorbed ligand throughout. The total amount of adsorbed ligand may be well-described as a function of time by a single decaying exponential function, that is, Eq. 19 with a single term. At high ligand concentration, and in the absence of adsorbate flipping (*bottom panel*), the reaction starts rapidly, and side-on conformation 1 binds preferentially, as would be expected. However, as the fractional surface coverage increases, $\text{rate}_{\text{soln}\rightarrow 1}$ begins to decrease relative to $\text{rate}_{\text{soln}\rightarrow 2}$, due to the enhanced increase of γ_1 relative to γ_2 with increasing surface coverage noted above, and becomes infinitesimal after about a hundredfold increase in elapsed time. Although at this point 1 is unstable thermodynamically relative to 2, it can have a very long lifetime if $\text{rate}_{1\rightarrow\text{soln}}$ and $\text{rate}^{\text{flip}}_{1\rightarrow 2}$ are small. As long as a significant fraction of the surface is occupied by 1, $\text{rate}_{\text{soln}\rightarrow 2}$, and hence the total rate of adsorption, will be greatly reduced relative to the rate expected in the absence of area exclusion. Under such conditions, even though conformation 1 represents a negligible fraction of total adsorbate at equilibrium, it can constitute a substantial kinetic barrier to the attainment of equilibrium. If the lifetime of 1 is suffi-

ciently long, the adsorption progress curve may exhibit a pre-equilibrium plateau (see below).

The effect of variation in flip rate on the kinetics of adsorption is illustrated in Fig. 12. As the flip rate increases, the lifetime of the transient side-on conformation is shortened and equilibrium is attained more rapidly. In the example shown, the bottom panel represents an asymptotic limit in which adsorbate conformations 1 and 2 equilibrate essentially instantaneously throughout the process of adsorption. Although adsorption under these conditions might be phenomenologically described as a combination of "fast" and "slow" phases, the two apparently kinetically distinguishable phases are in fact inextricably linked, and, as shown in the figure, neither can be well-modeled individually as an exponential function.

The effect of variation in free ligand concentration is illustrated in Fig. 13 in the limits of no flipping (*top panel*) and rapid flipping (*bottom panel*). In both limits, an increase in free ligand concentration enhances the separation of the "fast" and "slow" phases on the time scale, but in the fast flipping limit, the slower of the two phases is less retarded relative to the faster phase, and its apparent amplitude increased.

The effect of variation in J for constant L and Kc is illustrated in Fig. 14. As J increases, the "slow" phase is progressively retarded relative to the "fast" phase and the overall approach to equilibrium becomes increasingly stretched. The extent of stretching is enhanced in the absence of adsorbate flipping because the lifetime of conformation 1 is increased in accordance with Eq. 12. At sufficiently large values of J a nonequilibrium plateau of long duration appears in the adsorption progress curve. In the absence of kinetic data covering many orders of magnitude

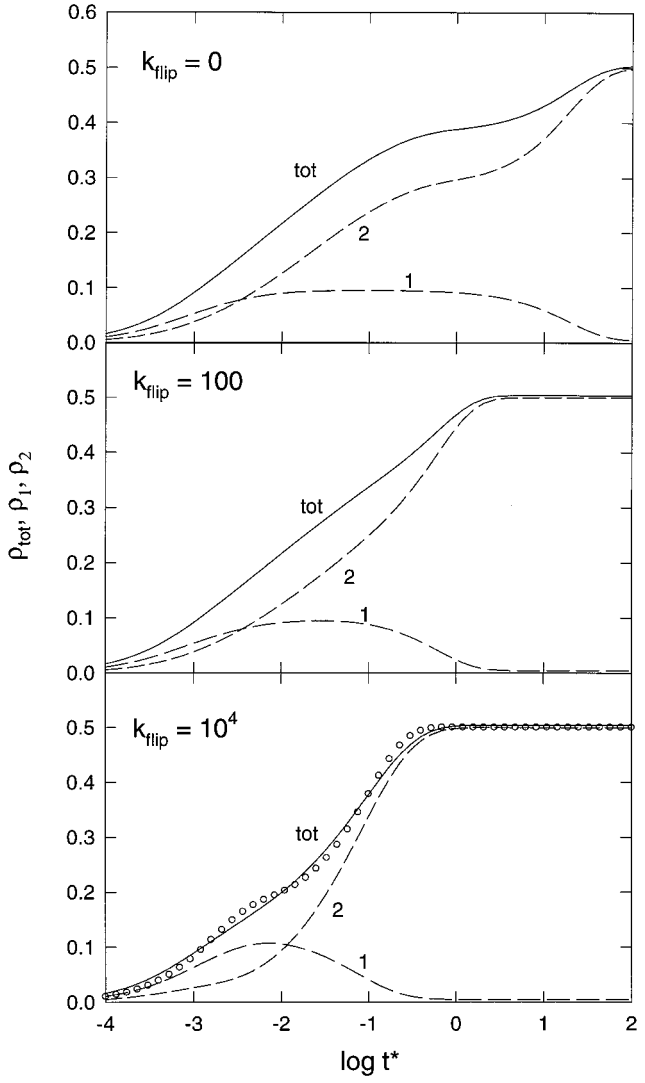

FIGURE 12 Effect of intrinsic conformational flipping rate on kinetic progress curves, calculated for $J = 1$, $L = 3$, $K_2c = 30$, and $K_{flip} = 0$ (*top panel*), 10^2 (*middle panel*), and 10^4 (*bottom panel*). The bottom panel corresponds to the asymptotic limit in which side-on and end-on adsorbates are in rapid equilibrium with each other throughout the adsorption process. Also plotted in this panel (*circular symbols*) is the calculated best-fit to the total progress curve of a two-term exponential expression of the form of Eq. 19.

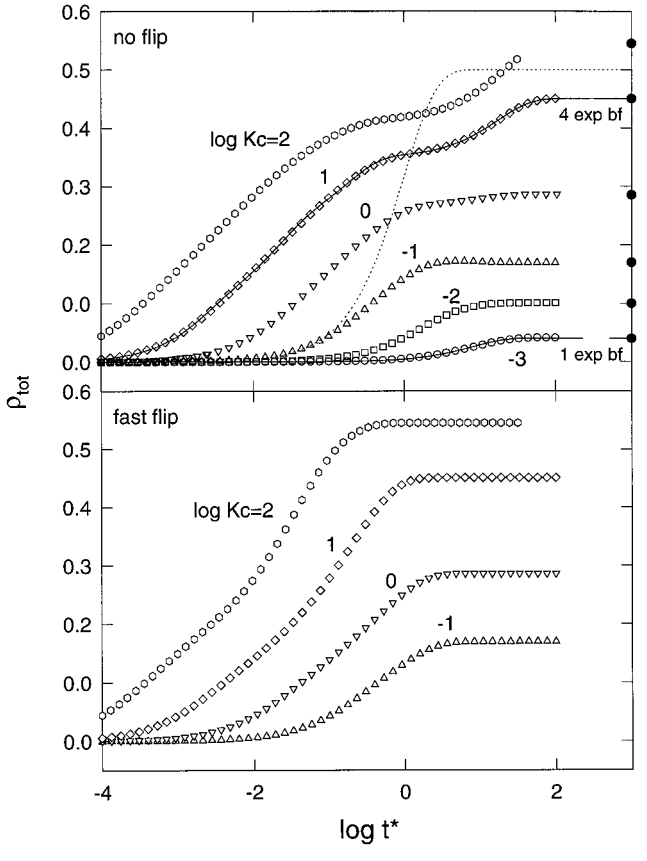

FIGURE 13 Effect of solution ligand concentration on kinetic progress curves, calculated for $J = 1$, $L = 3$, and the indicated values of K_2c in the limits of no conformational flipping (*top panel*) and fast conformational flipping (*bottom panel*). Also plotted in the upper panel are the amounts bound at equilibrium (*filled circles*), obtained from equilibrium results plotted in Fig. 5, a single exponential progress curve calculated according to the (ideal) Langmuir model for $K_2c = 1$, a single exponential best fit to the progress curve at $K_2c = 10^{-3}$, and a four-term exponential best fit to the progress curve at $K_2c = 10^2$.

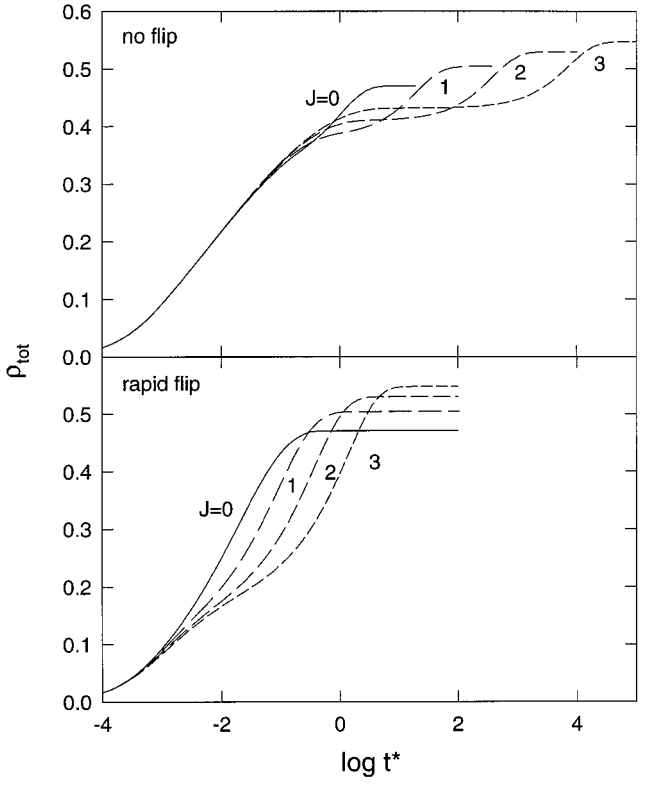

FIGURE 14 Effect of variation in intrinsic adsorption potential per unit surface area upon the kinetic progress curve in the limits of no conformational flipping (*top panel*) and rapid conformational flipping (*bottom panel*), calculated for $L = 3$, $K_2c = 30$, and $J = 0$, 1, 2, and 3 ("slow" phase of calculated curve shifts to right with increasing J).

in time, such a plateau could be reasonably (but mistakenly) taken to represent an equilibrium end-point. In the fast flipping limit, when the two adsorbate conformations are in continuous equilibrium, enhanced stretching is the result of an increase in the equilibrium constant K_{21} (Eq. 8) and a consequent shift to higher values of the fractional area occupancy at which conformation 2 becomes stable relative to conformation 1. For similar reasons, an increase in L at constant J is also expected to enhance stretching of the adsorption progress curve.

DISCUSSION

Although it is recognized that both repulsive and attractive interactions between adsorbed macromolecules play major roles in determining the shapes of equilibrium adsorption isotherms and kinetic progress curves (Nygren, 1993; Heimburg and Marsh, 1995; Kurrat et al., 1997; Wahlgren and Elofsson, 1997), relatively few attempts have been made to model such effects quantitatively. These attempts have fallen into two general classes, namely lattice simulations (Stenberg and Nygren, 1991; Jin, et al., 1994, Sild, et al., 1996) and continuum models based upon theories of two-dimensional fluids (Talbot, et al., 1994; Heimburg and Marsh, 1995; Chatelier and Minton, 1996; Talbot, 1997). Lattice model simulations provide straightforward means for calculating the probability of a particular configuration of the system (and hence estimating system entropy) as well as for the introduction of near-neighbor interactions between adsorbed particles (Stenberg and Nygren, 1991). The major disadvantage of such simulations is that a change in any parameter of the system requires a repetition of the entire simulation, which may be computationally costly and time-consuming. Moreover, lattice simulations may be subject to artifacts arising from the quantized representation of the system being modeled (see below). While continuum fluid models rely upon approximate theories of the fluid state, the numerical calculations are comparatively simple and quite rapid, and for the case of purely repulsive interactions between adsorbate molecules, the results of continuum model calculations of adsorption kinetics have been shown to agree quite well with the results of lattice simulations carried out using identical parameter values (Jin et al., 1994; Talbot et al., 1994).

Jin et al. (1994) have calculated $\phi(t)$ for uniformly sized hard disks adsorbing to a surface by using a semiempirical expression for $P(\phi)$ proposed earlier by Schaaf and Talbot (1989). Only very limited results are presented by these authors, and they are plotted as fractional surface area versus time rather than log t, hindering comparison over a broad time scale with the results presented here. However, we observe that in both studies the rate of slowing of the adsorption reaction with increasing surface occupancy is gradual rather than stepwise, i.e., does not exhibit multiphasic behavior that might be characteristic of separable exponential processes. Thus both the present results and those of Jin et al. (1994) stand in contrast to results presented by Sild et al. (1996), obtained via simulation on a lattice. These authors reported that the time-dependent adsorption of square ligands on a square lattice could be described a sum of two exponentials representing a relatively rapid process and a very slow process, the second of which was suggested to correspond to a "shuffling" of adsorbed ligands on the surface to make room for additional ligand. An exponential description of our own results for high ligand concentrations according to Eq. 19 requires four or five exponential terms rather than two (Fig. 10), and we can assign no physical significance to any individual term. We suggest that the "fast" exponential process reported by Sild et al. is, at least in part, an artifact arising from the unphysical orientational registration of square particles on a square lattice, which would tend to substantially reduce the area excluded by one adsorbed particle to another.

Talbot (1997) has very recently used scaled particle theory in a manner quite similar to that employed here to estimate the effect of area exclusion on the adsorption isotherm of a single molecular species that may adsorb in side-on and end-on conformations. Results qualitatively similar to those shown in the bottom panel of Fig. 4 were obtained. The present model represents an extension of Talbot's approach to allow for self-association (i.e., attractive as well as repulsive interactions between adsorbate

molecules) and to provide a description of rate processes as well as equilibria.

The existence of multiple interconvertible adsorbate conformations with different adsorption energies and surface footprints has the potential to significantly broaden the equilibrium adsorption isotherm along the concentration axis and the kinetic progress curve along the time axis. The progress curves plotted in Fig. 13 exhibit regions where binding increases linearly with the logarithm of time (to a good approximation) over as much as three orders of magnitude in time. Such nonclassical kinetics have been termed "fractal" (Nygren, 1993) although there does not seem to be any fractal aspect to the underlying mechanism in this particular instance.

Comparison of the results of model calculations, such as those presented here, with results obtained from experimental measurement of protein adsorption rates and equilibria is hindered by several complicating factors. An often-reported conclusion that a particular protein is absorbed irreversibly in part or in whole may be based upon the observation that the protein fails to dissociate substantially when exposed to protein-free solvent for a limited time period (see, for example, Brynda et al., 1986 and Schmitt et al., 1983). This interpretation neglects the "retention effect," i.e., the buildup and subsequent resorption of newly desorbed ligand in the unstirred layer immediately adjacent to the surface (Silhavy et al., 1975), which can profoundly slow the overall process of desorption. Even if means can be found to eliminate complications due to mass transport limitation of adsorption and desorption rates (Schuck, 1997), reversibility and/or attainment of equilibrium of a particular adsorption process may be extremely difficult to establish in a system exhibiting stretched kinetics resembling those indicated in Figs. 10–13. This is because kinetic data are ordinarily acquired and displayed at uniform intervals of time, where the size of the interval is dictated by the most rapidly changing (i.e., initial) part of the process (see, for example, Wahlgren, et al., 1995 and Kurrat et al., 1997). When represented on a constant time axis, even highly stretched kinetics appear to be describable (to within reasonable experimental error) over a limited range of time by an empirical expression of the form of Eq. 19 with one or two exponential terms, and the equilibrium adsorption estimated as the sum of the coefficients α_j. As shown in Fig. 15, this common procedure can lead to significant (20–40%) underestimates of the equilibrium value of ρ.

The results presented here also suggest the possibility that in contrast to the kinetic behavior predicted by the Langmuir model, large increases in free ligand concentration do not necessarily appreciably shorten the time required to attain adsorption equilibrium, which may in unfavorable cases be much larger than the duration of any reasonable experiment (see Note 10).

The adoption of surface-induced (i.e., nonsolution) conformations by adsorbed proteins is a very real possibility (Hummel and Anderson, 1965; Slack and Horbett, 1995). The present equilibrium model is compatible with such conformational change so long as surface-induced conformations are in reversible equilibrium with the solution conformation. In the present instance, any or all of the adsorbate conformations may be different from the solution conformation. No property of the equilibrium model depends upon the solution conformation, since the protein is assumed to behave ideally in solution, and any energy of conformational change upon adsorption may be subsumed into the adsorption potential. In contrast, the kinetic model would have to be generalized to allow for a rate (or rates) of conformational change following adsorption, and such generalization could conceivably stretch the progress curves still further.

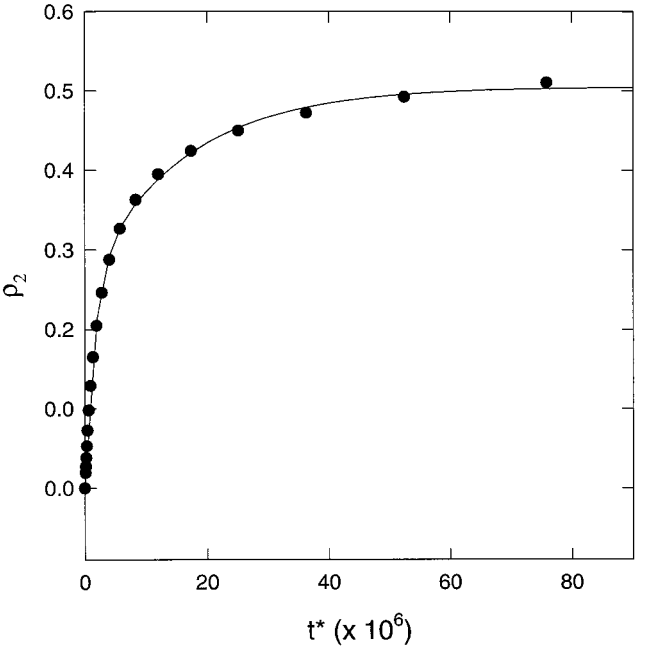

FIGURE 15 Replot on a linear time axis of a short-time subset of the time points plotted in the top panel of Fig. 10 ($K_2c = 10^5$). Also plotted (*solid line*) is the best fit to this truncated data set of a two-term exponential expression of the form of Eq. 19, which appears to the eye to be a satisfactory description of the data. The sum of the amplitudes of the two exponential terms is 0.505, whereas the total amount adsorbed at equilibrium (see Fig. 10) is 0.67.

Several globular proteins have been reported to attain maximum surface densities that are close to that calculated for hexagonal close packing of quasi-spherical particles with the same molar mass and density as the protein (Fig. 16). These observations suggest that at least some globular proteins retain a native or nativelike globular conformation upon adsorption, and that these proteins form large two-dimensional quasi-crystalline arrays. Such behavior would be consistent with the concept of adsorption-linked oligomerization or cluster formation (Ramsden et al., 1994; Minton, 1995). However, the process of formation of quasi-crystalline arrays must involve significant abundances of aggregates of intermediate size, as Langmuir-like adsorption isotherms reported in the literature (Al-Malah et al., 1995) are not consistent with those predicted by a simple

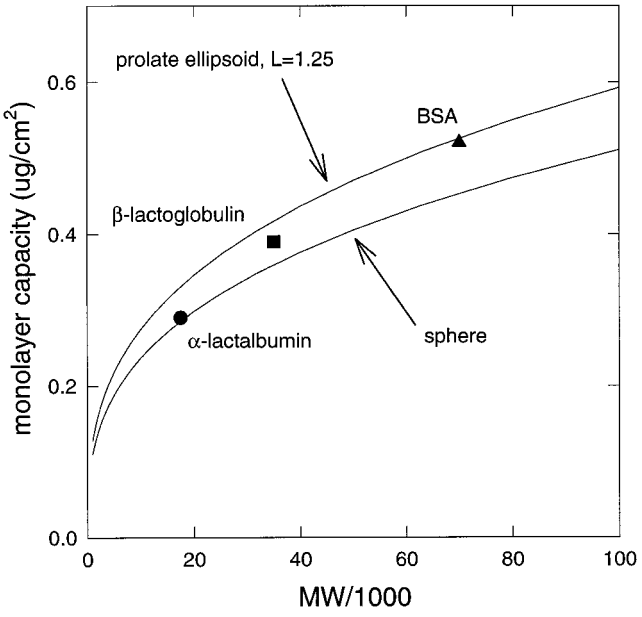

FIGURE 16 Experimentally measured monolayer capacity of α-lactalbumin, β-lactoglobulin, and BSA adsorbed to silanized silica surfaces (Al-Malah et al., 1995) plotted against molar mass of protein. Also shown are curves calculated for models in which adsorbed protein is represented by a hexagonal close-packed array of spheres or prolate ellipsoids of rotation (axial ratio 1.25, axis of rotation normal to the surface), and particle density taken to be 0.73 cm^3/g (i.e., equal to the average partial specific volume of protein).

three-state (solution monomer + adsorbed monomer + adsorbed *n*-mer) model when *n* is large (cf. Fig. 3 of CM). The kinetics and equilibria of multiassociation state adsorption models will be treated in a subsequent report.

NOTES

1. A surface is considered to be "flat" within the present context if irregularities in the direction normal to the surface plane are small relative to the smallest external dimension of the adsorbing ligand.

2. The number of equivalent ways in which a solution species can adsorb to the surface in a given orientation.

3. The selection of a single aggregate species with a square footprint is arbitrary and obviously oversimplified compared to any real aggregation process beyond dimer formation, which would probably involve multiple species of differing stoichiometry and footprints. The purpose of this model is simply to explore qualitative distinctions between adsorption isotherms in the presence and absence of adsorbate aggregation.

4. Copies of the MSDOS-executable program and Pascal source code are available upon request.

5. Consideration of the time-dependent formation/dissolution of adsorbed oligomers (e.g., species 3 in the equilibrium model) under highly area-excluded conditions is beyond the scope of the present work, because of the necessity of taking into account the possible existence of numerous additional kinetic intermediates.

6. The appropriateness of using scaled particle theory (or any other equilibrium equation of state) to calculate the instantaneous value of $P_i(\{\phi\})$ in a dynamically evolving system has been discussed by Talbot and co-workers (Jin et al., 1994; Talbot et al., 1994), who calculated that the difference between available area in irreversible and equilibrium conformations of hard particles randomly placed on a surface is probably smaller than the inexactness of the approximate equilibrium theories.

7. It may be readily shown that in the limit $d\rho_i/dt^* = 0$, Eq. 18 is consistent with the equilibrium relations (Eqs. 5 and 8).

8. A copy of the MLAB script file is available upon request.

9. In the present context the index *j* is phenomenological and does not necessarily represent the contribution of an individual molecular species or state to the overall adsorption process.

10. It is likely that at least some of the hysteresis curves reported to characterize adsorption of proteins (Jennisen, 1985; Norde and Haynes, 1995) are the result of a simple failure to attain equilibrium within the duration of the experiment, rather than an intrinsically irreversible mechanism of adsorption.

The author thanks Prof. K. Yutani and the staff and students of the Laboratory of Solution Chemistry, Institute for Protein Research, Osaka University, for their gracious hospitality and support during the tenure of a Visiting Professorship, June–August 1997, during which the work reported here was initiated.

REFERENCES

Al-Malah, K., J. McGuire, and R. Sproull. 1995. A macroscopic model for the single-component protein adsorption isotherm. *J. Colloid Interface Sci.* 170:261–268.

Boeynaems, J. M., and J. E. Dumont. 1980. Outlines of Receptor Theory. Elsevier/North-Holland, Amsterdam.

Brynda, E., M. Houska, and F. Lednicky. 1986. Adsorption of human fibrinogen onto hydrophobic surfaces: the effect of concentration in solution. *J. Colloid Interface Sci.* 113:164–171.

Chatelier, R. C., and A. P. Minton. 1996. Adsorption of globular proteins on locally planar surfaces: models for the effect of excluded surface area and aggregation of adsorbed protein on adsorption equilibria. *Biophys. J.* 71:2367–2374.

Heimburg, T., and D. Marsh. 1995. Protein surface distribution and protein-protein interactions in the binding of peripherial proteins to charged lipid membranes. *Biophys. J.* 68:536–546.

Hill, T. L. 1960. Introduction to Statistical Thermodynamics, Chap. 11. Addison-Wesley, Reading, MA.

Hummel, J. P., and B. S. Anderson. 1965. Ribonuclease adsorption on glass surfaces. *Arch. Biochem. Biophys.* 112:443–447.

Jennisen, H. P. 1985. Protein adsorption hysteresis. *In* Surface and Interfacial Aspects of Biomedical Polymers, Vol. 2. Plenum Press, NY. 295–320.

Jin, X., J. Talbot, and N.-H. L. Wang. 1994. Analysis of steric hindrance effects on adsorption kinetics and equilibria. *AIChE J.* 40:1685–1696.

Kurrat, R., J. E. Prenosil, and J. J. Ramsden. 1997. Kinetics of human and bovine serum adsorption at silica-titania surfaces. *J. Colloid Interface Sci.* 185:1–8.

Lebowitz, J. L., E. Helfand, and E. Praestgaard. 1965. Scaled particle theory of fluid mixtures. *J. Chem. Phys.* 43:774–779.

Minton, A. P. 1995. Confinement as a determinant of macromolecular structure and reactivity. II. Effects of weakly attractive interactions between confined macrosolutes and confining structures. *Biophys. J.* 68:1311–1322.

Norde, W., and C. A. Haynes. 1995. Reversibility and the mechanism of protein adsorption. *In* Proteins at Interfaces II. American Chemical Society, Washington, DC.

Nygren, H. 1993. Nonlinear kinetics of ferritin adsorption. *Biophys. J.* 65:1508–1512.

Ramsden, J. J., G. I. Bachmanova, and A. I. Archakov. 1994. Kinetic evidence for protein clustering at a surface. *Phys. Rev. E.* 50:5072–5076.

Roth, C. M., and A. M. Lenhoff. 1993. Electrostatic and van der Waals contributions to protein adsorption: computation of equilibrium constants. *Langmuir.* 9:962–972.

Roush, D. J., D. S. Gill, and R. C. Willson. 1994. Electrostatic potentials and electrostatic interaction energies of rat cytochrome b_5 and a simulated anion-exchange adsorbent surface. *Biophys. J.* 66:1290–1300.

Schaaf, P., and J. Talbot. 1989. Surface exclusion effects in adsorption processes. *J. Chem. Phys.* 91:4401–4409.

Schmitt, A., R. Varoqui, S. Uniyal, J. L. Brash, and C. Pusineri. 1983. Interaction of fibrinogen with solid surfaces of varying charge and hydrophobic-hydrophilic balance. I. Adsorption isotherms. *J. Colloid Interface Sci.* 92:25–34.

Schuck, P. 1997. Use of surface plasmon resonance to probe the equilibrium and dynamic aspects of interactions between biological macromolecules. *Annu. Rev. Biophys. Biomol. Struct.* 26:541–566.

Sild, V., J. Ståhlberg, G. Pettersson, and G. Johansson. 1996. Effect of potential binding site overlap to binding of cellulase to cellulose: a two-dimensional simulation. *FEBS Lett.* 378:51–56.

Silhavy, T. J., S. Szmelcman, W. Boos, and M. Schwartz. 1975. On the significance of the retention of ligand by protein. *Proc. Natl. Acad. Sci. USA.* 72:2120–2124.

Slack, S. M., and T. A. Horbett. 1995. The Vroman effect—a critical review. *In* Proteins at Interfaces II. American Chemical Society, Washington, D.C.

Stenberg, M., and H. Nygren. 1991. Computer simulation of surface-induced aggregation of ferritin. *Biophys. Chem.* 41:131–141.

Talbot, J. 1997. Molecular thermodynamics of binary mixture adsorption: a scaled particle theory approach. *J. Chem. Phys.* 106:4696–4706.

Talbot, J., X. Jin, and N.-H. L. Wang. 1994. New equations for multicomponent adsorption kinetics. *Langmuir.* 10:1663–1666.

Wahlgren, M., T. Arnebrant, and I. Lundstron. 1995. Adsorption of lysozyme to hydrophilic silicon oxide surfaces: comparison between experimental data and models for adsorption kinetics. *J. Colloid Interface Sci.* 175:506–514.

Wahlgren, M., and U. Elofsson. 1997. Simple models for adsorption kinetics and their correlation to the adsorption of β-lactoglobulin A and B. *J. Colloid Interface Sci.* 188:121–129.

Zimmerman, S., and A. P. Minton. 1993. Macromolecular crowding: biochemical, biophysical and physiological consequences. *Annu. Rev. Biophys. Biomol. Struct.* 22:27–65.